

Nodeless superconductivity in $\text{Ca}_3\text{Ir}_4\text{Sn}_{13}$: evidence from quasiparticle heat transport

S. Y. Zhou, H. Zhang, X. C. Hong, B. Y. Pan, X. Qiu, W. N. Dong, X. L. Li, and S. Y. Li*

*State Key Laboratory of Surface Physics, Department of Physics,
and Laboratory of Advanced Materials, Fudan University, Shanghai 200433, P. R. China*

(Dated: February 17, 2019)

We report thermal conductivity measurements down to 50 mK on $\text{Ca}_3\text{Ir}_4\text{Sn}_{13}$ single crystals, in which superconductivity with $T_c \approx 7$ K was claimed to coexist with ferromagnetic spin-fluctuations. In zero magnetic field, no residual linear term κ_0/T is found. In low magnetic fields, $\kappa_0(H)/T$ shows a slow field dependence. These results demonstrate that the superconducting gap of $\text{Ca}_3\text{Ir}_4\text{Sn}_{13}$ is nodeless, thus rule out an exotic nodal gap caused by ferromagnetic spin-fluctuations. The relatively fast increase of $\kappa_0(H)/T$ near the upper critical field H_{c2} may result from gap anisotropy, or multiple isotropic gaps with different magnitudes.

PACS numbers: 74.25.fc, 74.70.Dd

I. INTRODUCTION

The interplay between magnetism and superconductivity has been a central issue in unconventional superconductors. While the static magnetism is generally believed to compete with superconductivity, the dynamic magnetism could be the source of electron pairing.¹ For example, the antiferromagnetic (AF) spin-fluctuations are considered as the pairing glue in high- T_c cuprates, iron-based superconductors, and many heavy-fermion superconductors.¹ On another side, the ferromagnetic (FM) spin-fluctuations could be the origin of the superconductivity in Sr_2RuO_4 , heavy-fermion superconductors UGe_2 and URhGe .¹ These AF and FM spin-fluctuations usually result in superconducting gaps with nodes, such as the d -wave gap in cuprates and CeCoIn_5 ,^{2,3} and the p -wave gap in Sr_2RuO_4 .⁴

$\text{Ca}_3\text{Ir}_4\text{Sn}_{13}$ is a cubic transition metal compound, in which superconductivity with $T_c \approx 7$ K was found thirty years ago.⁵ Very few studies have been done on this compound since its discovery. Until recently, detailed resistivity, susceptibility, and specific heat measurements suggested that the superconductivity coexists with the FM spin-fluctuations in $\text{Ca}_3\text{Ir}_4\text{Sn}_{13}$.⁶ The non-Fermi-liquid behavior of resistivity in zero field has been attributed to such spin-fluctuations, and upon applying magnetic field, Fermi liquid behavior is recovered.⁶

Since the FM spin-fluctuations may cause an exotic superconducting state in $\text{Ca}_3\text{Ir}_4\text{Sn}_{13}$, it will be interesting to probe its superconducting gap structure. Ultra-low-temperature thermal conductivity measurement is such a bulk technique.⁷ The existence of a finite residual linear term κ_0/T in zero magnetic field is a clear evidence for gap nodes. The field dependence of κ_0/T may further give support for a nodal superconducting state, and provide informations on the gap anisotropy, or multiple gaps.⁸

In this Brief Report, we measure the low-temperature thermal conductivity of $\text{Ca}_3\text{Ir}_4\text{Sn}_{13}$ single crystals down to 50 mK. The absence of κ_0/T in zero field and the slow field dependence of $\kappa_0(H)/T$ in low fields clearly demonstrate nodeless superconductivity in $\text{Ca}_3\text{Ir}_4\text{Sn}_{13}$.

The relatively fast increase of $\kappa_0(H)/T$ near the upper critical field H_{c2} is discussed.

II. EXPERIMENT

Single crystals of $\text{Ca}_3\text{Ir}_4\text{Sn}_{13}$ were grown by flux method, as previously described in Ref. 5. The excessive Sn flux was etched in concentrated hydrochloric acid (HCl). The obtained single crystals have typical size of a few mm^3 . We chose a single crystal with a large surface, which was determined as (110) plane by X-ray diffraction measurements. Then the single crystal was polished and cut to a rectangular shape of dimensions $2.5 \times 1.8 \text{ mm}^2$ in the (110) plane, and 0.22 mm in thickness. The dc magnetic susceptibility was measured at $H = 20$ Oe, with zero-field cooled, using a SQUID (MPMS, Quantum Design). Four silver wires were attached on the sample with silver paint, which were used for both resistivity and thermal conductivity measurements, with electrical and heat currents in the (110) plane. The contacts are metallic with typical resistance 50 m Ω at 2 K. The thermal conductivity was measured in a dilution refrigerator, using a standard four-wire steady-state method with two RuO_2 chip thermometers, calibrated *in situ* against a reference RuO_2 thermometer. Magnetic fields were applied perpendicular to the (110) plane. To ensure a homogeneous field distribution in the sample, all fields were applied at temperature above T_c .

III. RESULTS AND DISCUSSION

Figure 1(a) presents the normalized dc magnetization of $\text{Ca}_3\text{Ir}_4\text{Sn}_{13}$ single crystal, measured in $H = 20$ Oe with zero-field cooled condition. The transition temperature $T_c = 6.85$ K is determined from the onset of diamagnetic transition. Fig. 1(b) plots the low-temperature resistivity of $\text{Ca}_3\text{Ir}_4\text{Sn}_{13}$ single crystal in $H = 0$ T. The zero-resistivity $T_c = 6.95$ K is roughly the same as that obtained from the magnetization measurement in Fig.

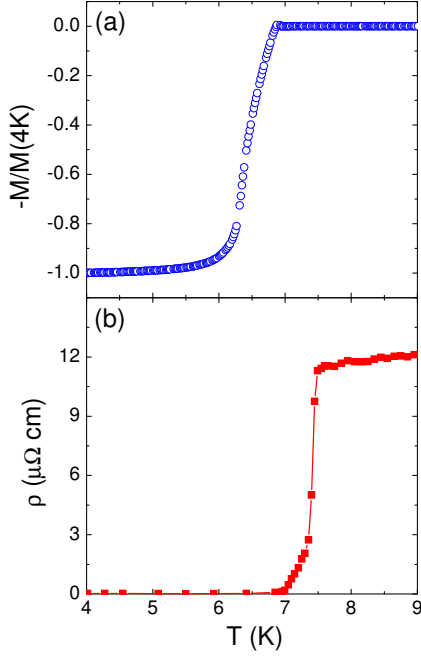


FIG. 1: (Color online) (a) Normalized dc magnetization of $\text{Ca}_3\text{Ir}_4\text{Sn}_{13}$ single crystal, measured at $H = 20$ Oe with zero-field cooled. (b) Resistivity of $\text{Ca}_3\text{Ir}_4\text{Sn}_{13}$ single crystal in zero magnetic field. The zero-resistivity transition temperature $T_c = 6.95$ K is very close to the $T_c = 6.85$ K determined from the onset of the diamagnetic transition in (a).

1(a). The 10-90% resistive transition width is 0.3 K. These results are consistent with Ref. 6.

Figure 2(a) shows the resistivity of $\text{Ca}_3\text{Ir}_4\text{Sn}_{13}$ single crystal in magnetic field up to $H = 7$ T. For $H = 6$ and 7 T, no superconducting transition is observed down to 2 K. The normal-state $\rho(7\text{T})$ curve is quite flat, extrapolating to a residual resistivity $\rho_0(7\text{T}) \approx 16.4 \mu\Omega \text{ cm}$. This value is lower than that reported in Ref. 6, indicating that our single crystal may have higher quality. In Fig. 2(b), we plot the temperature dependence of the upper critical field H_{c2} , defined by $\rho = 0$ from the curves in Fig. 1(a). A rough estimation gives $H_{c2}(0) \approx 7$ T, the same as in Ref. 6.

Figure 3 shows the temperature dependence of the thermal conductivity for $\text{Ca}_3\text{Ir}_4\text{Sn}_{13}$ single crystal in $H = 0, 2, 3, 4, 5, 6$, and 7 T magnetic fields, plotted as κ/T vs T . The measured thermal conductivity is the sum of two contributions, respectively from electrons and phonons, so that $\kappa = \kappa_e + \kappa_p$. In order to obtain the residual linear term κ_0/T contributed by electrons, we extrapolate κ/T to $T = 0$. Usually, this can be done by fitting the data to $\kappa/T = a + bT^\alpha$ at low temperature, where $a \equiv \kappa_0/T$.^{9,10} The power α of the second term contributed by phonons is typically between 2 and 3.^{9,10} From Fig. 3, all the curves are roughly linear, therefore we fit the data to $\kappa/T = a + bT^\alpha$ with α fixed at 2. Previously $\alpha \approx 2.2$ has been observed in the s -wave superconductor $\text{Cu}_{0.06}\text{TiSe}_2$,¹¹ and recently $\alpha \approx 2$

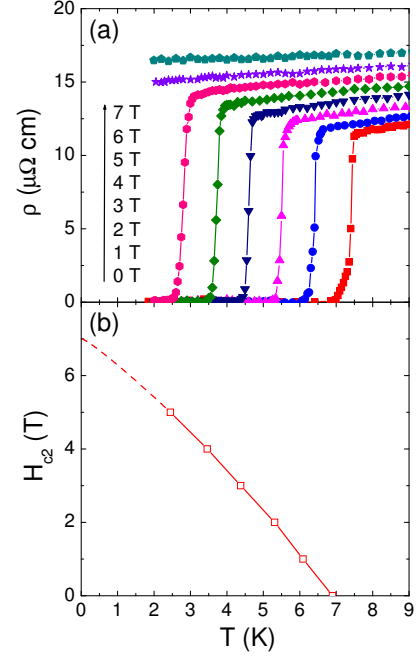


FIG. 2: (Color online) (a) Resistivity of $\text{Ca}_3\text{Ir}_4\text{Sn}_{13}$ single crystal in $H = 0, 1, 2, 3, 4, 5, 6$, and 7 T. The normal-state $\rho(7\text{T})$ curve is quite flat, extrapolating to residual resistivity $\rho_0(7\text{T}) \approx 16.4 \mu\Omega \text{ cm}$. (b) Temperature dependence of the upper critical field H_{c2} , defined by $\rho = 0$. The dashed line is a guide to the eye, which points to $H_{c2}(0) \approx 7$ T.

was found in some iron-based superconductors such as $\text{BaFe}_{1.9}\text{Ni}_{0.1}\text{As}_2$ and KFe_2As_2 .^{12,13} In Fig. 3, from zero field to $H = 2$ T, there is an increase of the slope b in the second term bT^α . With further increasing field, the slope b gradually decreases. At this stage the reason for the increase of b at low field is not clear to us. Below we only focus on the residual linear term κ_0/T .

In zero field, the fitting gives $\kappa_0/T = -0.007 \pm 0.004 \text{ mW K}^{-2} \text{ cm}^{-1}$. For s -wave nodeless superconductors, there are no fermionic quasiparticles to conduct heat as $T \rightarrow 0$, since all electrons become Cooper pairs. Therefore there is no residual linear term of κ_0/T , as seen in V_3Si .⁹ However, for unconventional superconductors with nodes in the superconducting gap, the nodal quasiparticles will contribute a finite κ_0/T in zero field.⁷ For example, $\kappa_0/T = 1.41 \text{ mW K}^{-2} \text{ cm}^{-1}$ for the overdoped cuprate $\text{Tl}_2\text{Ba}_2\text{CuO}_{6+\delta}$ (Tl-2201), a d -wave superconductor with $T_c = 15$ K.¹⁸ For the p -wave superconductor Sr_2RuO_4 , $\kappa_0/T = 17 \text{ mW K}^{-2} \text{ cm}^{-1}$.¹⁴ Therefore, the negligible residual linear term in $\text{Ca}_3\text{Ir}_4\text{Sn}_{13}$ strongly suggests that its superconducting gap is nodeless, thus rules out a nodal gap caused by FM spin-fluctuations.

In $H_{c2} = 7$ T, $\kappa_0/T = 1.51 \pm 0.02 \text{ mW K}^{-2} \text{ cm}^{-1}$ was obtained from the fitting. This value meets the Wiedemann-Franz law expectation $L_0/\rho_0(7\text{T}) = 1.49 \text{ mW K}^{-2} \text{ cm}^{-1}$ within experimental error bar, with L_0 the Lorenz number $2.45 \times 10^{-8} \text{ W}\Omega\text{K}^{-2}$ and normal-state $\rho_0(7\text{T}) = 16.4 \mu\Omega \text{ cm}$. The verification of

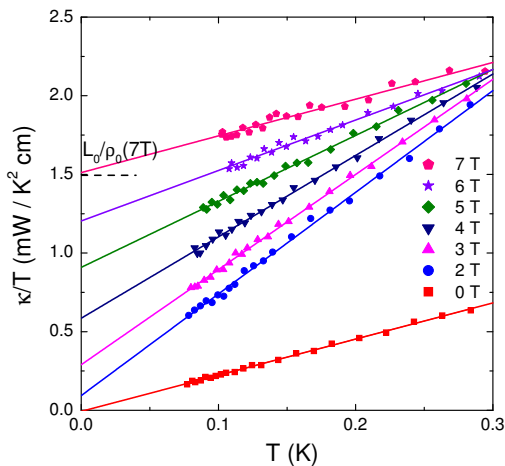


FIG. 3: (Color online) Low-temperature thermal conductivity of $\text{Ca}_3\text{Ir}_4\text{Sn}_{13}$ single crystal, with heat current in the (110) plane, in zero and magnetic fields applied perpendicular to the (110) plane. The solid lines are $\kappa/T = a + bT$ fit to all the curves, respectively. The dash line is the normal-state Wiedemann-Franz law expectation $L_0/\rho_0(7\text{T})$, with L_0 the Lorenz number $2.45 \times 10^{-8} \text{ W}\Omega\text{K}^{-2}$ and normal-state $\rho_0(7\text{T}) = 16.4 \mu\Omega \text{ cm}$.

Wiedemann-Franz law in the normal state shows the reliability of our thermal conductivity measurements.

As seen in Fig. 3, κ_0/T gradually increases with increasing field. In Fig. 4, we plot the normalized $\kappa_0(H)/T$ as a function of H/H_{c2} for $\text{Ca}_3\text{Ir}_4\text{Sn}_{13}$, together with the clean s -wave superconductor Nb,¹⁵ the dirty s -wave superconducting alloy InBi,¹⁶ the multi-band s -wave superconductor NbSe₂,¹⁷ and an overdoped sample of the d -wave superconductor Tl-2201.¹⁸ For a clean type-II s -wave superconductor with a single gap, κ should grow exponentially with field (above H_{c1}), as is indeed observed in Nb.¹⁵ For InBi, the curve is exponential at low H , crossing over to a roughly linear behavior closer to H_{c2} as expected for s -wave superconductors in the dirty limit.¹⁹

The normalized $\kappa_0(H)/T$ of $\text{Ca}_3\text{Ir}_4\text{Sn}_{13}$ clearly mimics that of the dirty s -wave superconductor InBi. However, previously Yang *et al.* estimated the superconducting coherence length $\xi_0 \sim 79 \text{ \AA}$ and electronic mean free path $l \sim 811 \text{ \AA}$, which implies that $\text{Ca}_3\text{Ir}_4\text{Sn}_{13}$ is an intrinsic clean-limit superconductor ($\xi_0 \ll l$).⁶ Since the ρ_0 of our single crystal is lower than that of Yang *et al.*'s, our sample is cleaner than theirs. Therefore, the relatively fast increase of $\kappa_0(H)/T$ near H_{c2} in $\text{Ca}_3\text{Ir}_4\text{Sn}_{13}$ should have different origin from the dirty s -wave superconductor InBi.

Band structure calculation shows that there are six bands in $\text{Ca}_3\text{Ir}_4\text{Sn}_{13}$ which cross the Fermi level.²³ Each sheet of the Fermi surface was found to be three dimensional, with rather complex shape.²³ In this context, we interpret the $\kappa_0(H)/T$ behavior of $\text{Ca}_3\text{Ir}_4\text{Sn}_{13}$ may result from multiple gaps or gap anisotropy.

For the multi-band s -wave superconductor NbSe₂,

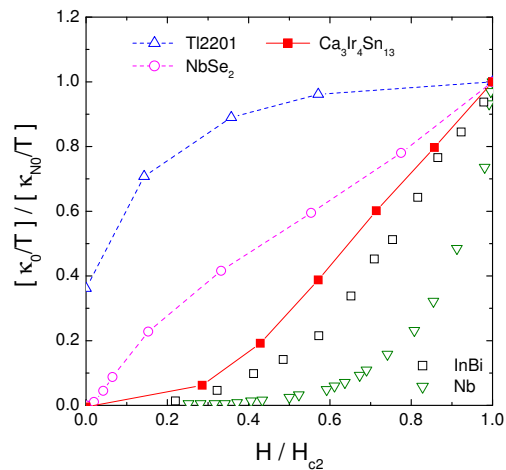


FIG. 4: (Color online) Normalized residual linear term κ_0/T of $\text{Ca}_3\text{Ir}_4\text{Sn}_{13}$ plotted as a function of H/H_{c2} . For comparison, similar data are shown for the clean s -wave superconductor Nb,¹⁵ the dirty s -wave superconducting alloy InBi,¹⁶ the multi-band s -wave superconductor NbSe₂,¹⁷ and an overdoped sample of the d -wave superconductor Tl-2201.¹⁸

$\kappa_0(H)/T$ increases rapidly in both low field and near H_{c2} .¹⁷ Similar behavior has been observed in $\text{LNi}_2\text{B}_2\text{C}$ ($L = \text{Y, Lu}$) with multiple and anisotropic gaps.^{20,21} In both NbSe₂ and $\text{LNi}_2\text{B}_2\text{C}$, applying a field rapidly delocalizes quasiparticle states confined within the vortices associated with the smaller gap band, while those states associated with the larger gap band delocalize more slowly. For NbSe₂, the ratio between larger and smaller gaps is approximately 3,²² and for $\text{YNi}_2\text{B}_2\text{C}$, the ratio is about 2.1.²¹ Recently, Bang has calculated the field dependence of $\kappa_0(H)/T$ for different gap ratios, to explain the thermal conductivity data of multi-gap iron-based superconductor $\text{Ba}(\text{Fe}_{1-x}\text{Co}_x)_2\text{As}_2$.²⁴ It is possible that in $\text{Ca}_3\text{Ir}_4\text{Sn}_{13}$, the gaps in the six Fermi surfaces may have different magnitudes, or in some Fermi surface the gap is anisotropic. If this is the case, according to Bang's calculation,²⁴ the gap ratio in $\text{Ca}_3\text{Ir}_4\text{Sn}_{13}$ should be around 1.4 or so. This interpretation needs to be checked by momentum dependent measurements of the superconducting gap, such as anglesolved photoemission spectroscopy (ARPES) experiments.

IV. SUMMARY

In summary, we report the ultra-low-temperature thermal conductivity measurements of $\text{Ca}_3\text{Ir}_4\text{Sn}_{13}$ single crystals. Despite that FM spin-fluctuations were claimed to exist in this superconductor, our thermal conductivity results clearly show that its superconducting gap is nodeless. This implies that the FM spin-fluctuations may be irrelevant to the superconductivity in $\text{Ca}_3\text{Ir}_4\text{Sn}_{13}$, and the conventional electron-phonon interaction should be responsible for the electron pairing. The $\kappa_0(H)/T$ shows

a relatively fast increase near H_{c2} . Since $\text{Ca}_3\text{Ir}_4\text{Sn}_{13}$ is not in the dirty limit, but rather has multiple Fermi surfaces with complex shape, we interpret that the behavior of $\kappa_0(H)/T$ may result from gap anisotropy, or multiple isotropic gaps with different magnitudes.

ACKNOWLEDGEMENTS

This work is supported by the Natural Science Foundation of China, the Ministry of Science and

Technology of China (National Basic Research Program No: 2009CB929203 and 2012CB821402), Program for Professor of Special Appointment (Eastern Scholar) at Shanghai Institutions of Higher Learning.

* E-mail: shiyan_li@fudan.edu.cn

-
- ¹ M. R. Norman, Science **332**, 196 (2011), and references therein.
 - ² C. C. Tsuei and J. R. Kirtley, Rev. Mod. Phys. **72**, 969 (2000).
 - ³ K. An, T. Sakakibara, R. Settai, Y. Onuki, M. Hiragi, M. Ichioka, and K. Machida, Phys. Rev. Lett. **104**, 037002 (2010).
 - ⁴ A. P. Mackenzie and Y. Maeno, Rev. Mod. Phys. **75**, 657 (2003).
 - ⁵ G. P. Espinosa, Mater. Res. Bull. **15**, 791 (1980). G. P. Espinosa, A. S. Copper, and H. Barz, Mater. Res. Bull. **17**, 963 (1982).
 - ⁶ Jinhu Yang, Bin Chen, Chishiro Michioka, and Kazuyoshi Yoshimura, J. Phys. Soc. Jpn. **19**, 113705 (2010).
 - ⁷ H. Shakeripour, C. Petrovic, and L. Taillefer, New J. Phys. **11**, 055065 (2009).
 - ⁸ R. W. Hill, Shiyan Li, M. B. Maple, and Louis Taillefer, Phys. Rev. Lett. **101**, 237005 (2008).
 - ⁹ M. Sutherland, D. G. Hawthorn, R. W. Hill, F. Ronning, S. Wakimoto, H. Zhang, C. Proust, E. Boaknin, C. Lupien, and Louis Taillefer, Phys. Rev. B **67**, 174520 (2003).
 - ¹⁰ S. Y. Li, J.-B. Bonnemaïson, A. Payeur, P. Fournier, C. H. Wang, X. H. Chen, and L. Taillefer, Phys. Rev. B **77**, 134501 (2008).
 - ¹¹ S. Y. Li, G. Wu, X. H. Chen, and Louis Taillefer, Phys. Rev. Lett. **99**, 107001 (2007).
 - ¹² L. Ding, J. K. Dong, S. Y. Zhou, T. Y. Guan, X. Qiu, C. Zhang, L. J. Li, X. Lin, G. H. Cao, Z. A. Xu and S. Y. Li, New J. Phys. **11**, 093018 (2009).
 - ¹³ J. K. Dong, S. Y. Zhou, T. Y. Guan, H. Zhang, Y. F. Dai, X. Qiu, X. F. Wang, Y. He, X. H. Chen, and S. Y. Li, Phys. Rev. Lett. **104**, 087005 (2010).
 - ¹⁴ M. Suzuki, M. A. Tanatar, N. Kikugawa, Z. Q. Mao, Y. Maeno, and T. Ishiguro, Phys. Rev. Lett. **88**, 227004 (2002).
 - ¹⁵ J. Lowell and J. B. Sousa, J. Low. Temp. Phys. **3**, 65 (1970).
 - ¹⁶ J. O. Willis and D. M. Ginsberg, Phys. Rev. B **14**, 1916 (1976).
 - ¹⁷ E. Boaknin, M. A. Tanatar, J. Paglione, D. Hawthorn, F. Ronning, R. W. Hill, M. Sutherland, Louis Taillefer, J. Sonier, S. M. Hayden, and J. W. Brill, Phys. Rev. Lett. **90**, 117003 (2003).
 - ¹⁸ C. Proust, E. Boaknin, R. W. Hill, Louis Taillefer, and A. P. Mackenzie, Phys. Rev. Lett. **89**, 147003 (2002).
 - ¹⁹ C. Caroli and M. Cyrot, Phys. Kondens. Mater. **4**, 285 (1965).
 - ²⁰ E. Boaknin, R. W. Hill, C. Proust, C. Lupien, Louis Taillefer, and P. C. Canfield, Phys. Rev. Lett. **87**, 237001 (2001).
 - ²¹ T. Baba, T. Yokoya, S. Tsuda, T. Watanabe, M. Nohara, H. Takagi, T. Oguchi, and S. Shin, Phys. Rev. B **81**, 180509(R) (2010).
 - ²² T. Yokoya, T. Kiss, A. Chainani, S. Shin, M. Nohara, H. Takagi, Science **294**, 2518 (2001).
 - ²³ S. K. Goh, L. E. Klintberg, P. L. Alireza, D. A. Tompsett, Jinhu Yang, Bin Chen, K. Yoshimura, and F. Malte Grosche, arXiv:1105.3941 (2011).
 - ²⁴ Yunkyu Bang, Phys. Rev. Lett. **104**, 217001 (2010).